Reac Kinet Mech Cat (2014) 112:527–542
DOI 10.1007/s11144-014-0703-5

Photodegradation of methylene blue over novel 3D ZnO microflowers with hexagonal pyramid-like petals

Manoj Pudukudy · Zahira Yaakob · Ramesh Rajendran · Thushara Kandaramath

Received: 29 January 2014 / Accepted: 16 March 2014 / Published online: 5 April 2014

Abstract Three dimensional ZnO microflowers with a huge number of hexagonal pyramid-like petals have been effectively synthesized via the thermal decomposition of previously melted nitrate precursor for the first time. The synthesis was done without the aid of any structure directing agents or templates. Powder X-ray diffraction patterns showed the hexagonal wurtzite crystalline structure of ZnO with high phase purity. The dimension of the large microflower noted was found to be around 100 μm with the simultaneous existence of small flowers, with size varying from 20 μm onwards as realized from the scanning electron microscopic images. Transmission electron microscopy and selected area electron diffraction patterns confirmed the oriented growth of the single crystalline basic hexagonal pyramidal units of the microflower for its oriented aggregation. A possible growth/formation mechanism was interpreted. The photocatalytic degradation of methylene blue was investigated over ZnO microflowers. ZnO microflowers showed its excellent photocatalytic activity in the degradation of several industrial dye pollutants over a low catalyst dosage under UV-light irradiation. The microflowers were found to be highly reusable for repeated degradation of methylene blue dye pollutant.

Keywords ZnO microflowers · Pyramidal petals · Thermal decomposition · Photodegradation · Methylene blue

M. Pudukudy
Fuel Cell Institute, Universiti Kebangsaan Malaysia, UKM, 43600 Bangi, Selangor, Malaysia

M. Pudukudy · Z. Yaakob (✉) · R. Rajendran · T. Kandaramath
Department of Chemical and Process Engineering, Faculty of Engineering and Built Environment, Universiti Kebangsaan Malaysia, UKM, 43600 Bangi, Selangor, Malaysia
e-mail: zahirayaakob65@gmail.com

Introduction

The controlled assembly of nanomaterials to well-defined structures often results in excellent properties of materials, applicable in electronics, photonics and in catalysis [1]. The well-oriented growth of nanoparticles to form attractive morphologies is an art in the material synthesis [2]. Advanced techniques such as the sol-gel route, hydrothermal method, homogeneous precipitation route etc. were succeeded in this context with and without the assistance of structure directing agents [3]. Tedious procedures, careful control of parameters, difficulty in the large scale production etc. make some of the synthesis routes highly tiresome. The high cost of the whole process is the main hurdle faced for the achievement of nanostructures with novel morphologies and properties. Attainment of a simple and effective synthesis route to overtake the aforementioned complications has caught much special attention in materials science. ZnO is an important n-type semiconductor with high performance in a wide variety of applications such as in optoelectronic devices, pyroelectric devices, piezoelectric devices, self-compensating gas sensors, high power electronic devices, surface acoustic wave devices, field effect transistors, low threshold optical pumping devices, substrate transparent electrodes etc. [4–8]. The band gap of ZnO lies in the UV region (3.37 eV), so that it is applied in solar cells, self-cleaning devices, sun screen lotions and also in photocatalysis [9–13].

There are several reports on the synthesis and characterization of nano- and micro-structured ZnO particles with versatile properties [14–17]. The common synthesis methods, i.e. the solution-based wet methods and the physical methods were successfully employed for the synthesis of ZnO nanostructures. The physical methods such as chemical vapor deposition [18], spray pyrolysis [19] etc. have been used in the formation of high quality inorganic nanostructures, but a low final yield was noted; as well as the fact that it needs high temperatures and pressures. In addition, costly equipment was needed to process it. The solution-based wet techniques include the sol–gel method, precipitation method, solvothermal, hydrothermal, microemulsion etc. and those which additionally use surfactants or templates for the structure and morphology development [20–26].

The formation of novel morphologies as a result of the solution-based techniques is comparatively convenient, facile and is applied on large scales since these are economically viable. Still, these techniques often require specific requirements associated with synthesis procedures such as control of pH, temperatures, pressures, use of costly structural modifiers, requirement of special equipments etc. [27]. Therefore, the development of a preparation method for novel ZnO structures with a simplified procedure is highly desirable in materials science. The synthesis of size and morphology controlled ZnO particles is a challenging task in the area of current materials research. Thermal decomposition is the one of the most promising methods for the preparation of nano/micro structured materials. Previously, it has been reported that ZnO nanoparticles with a particular morphology can be achieved by the thermal treatment of precursors with organic additives [28–32] and the nature of solvent used in those synthesis has a crucial role in the morphology of ZnO nanomaterials [33].

In recent years, numerous studies were carried out on the photocatalytic activities of ZnO nanoparticles with various morphologies like nanowires, nanorods, nanotubes, micro and nanoflowers etc. [34–39]. From this discussion, it is understood that the preparation of morphology regulated ZnO photocatalysts without the use of any organic modifiers or surfactants is highly demanding. Few studies have been reported for the synthesis of highly photoactive ZnO nanostructures by the direct thermal decomposition method. Saravanan et al. [40] prepared ZnO nanorods by the direct thermal decomposition of acetate precursor and investigated its photocatalytic activity for the degradation of textile dyes.

In the present work, three dimensional ZnO microflowers were synthesized by the pyrolysis of previously grinded/melted precursor, zinc(II) nitrate hexahydrate, without the aid of any organic modifiers and structure directing agents. To the best of our knowledge, this is the first report for the synthesis of three dimensional ZnO microflowers containing a large number of hexagonal pyramid like petals by an easily performable pyrolysis, the simplest technique of material synthesis. The photocatalytic activity of as-synthesised ZnO microflowers was studied for the degradation of dye molecules.

Experimental details

Synthesis of ZnO microflowers

Thermal decomposition of a nitrate precursor was employed for the material preparation. In the typical experiment, a weighed amount of zinc(II) nitrate hexahydrate (R&M chemicals, UK) was ground and pulverized in a mortar using a pestle. Subsequently, it was transferred to a large quartz crucible and kept in air contact till it become free flowing form (i.e. watery form due to the hygroscopic nature and melting of the sample during pulverization) and calcined at two temperatures (400 and 600 °C) in a muffle furnace for 4.5 h to obtain ZnO microflowers.

Characterization

The as-synthesized ZnO materials were subjected to structural and morphological analysis using different techniques. Thermogravimetric and differential scanning calorimetric analysis (TG/DSC) of the treated nitrate precursor was done in a thermogravimetric analyzer (STA 449 F3 JUPITER) with helium carrier gas. Powder X-ray diffraction (XRD) analysis of the samples was performed on a Bruker D8 ADVANCE powder diffractometer with Cu K_α radiation wavelength of 0.15406 nm. The samples were scanned from 3° to 80° with 0.025° step size. The crystalline size for each sample was calculated from the full width at the half maximum of the X-ray diffraction peak at around 36° using the Scherrer equation (processed data). Fourier transform infrared spectra (FT-IR) of the calcined products were recorded in transmission mode using Thermo Scientific NICOLET 6,700 in the region of 400–4,000 cm^{-1}. Scanning electron microscopy (SEM)

images of the materials were taken using Carl Zeiss Evo Ma10 VPSEM instrument and the electron micrographs were obtained at an operating voltage of 10 kV. Transmission electron microscopy (TEM) images were taken by a Philips CM-12 instrument with an operating voltage of 100 kV. Selected area electron diffraction (SAED) analysis was taken using a Hitachi 120 kV TEM HT-7700 instrument.

Photocatalytic measurements

The photocatalytic activity of the as-synthesized ZnO microflowers was investigated using methylene blue (MB) degradation under UV-light irradiation in a Rayonet type photoreactor (Associate Technica, India) with 16 tubes of 8 W UV lamps, with an irradiation wavelength of 352 nm (HITACHI F8T5 8 WATT Hittach, Ltd. Tokyo Japan, Made in Japan). Methylene blue dye solution (50 mL) with a fixed concentration (5 mg/L) was taken in a tubular vessel having a total capacity of 110 mL and weighed amount of ZnO photocatalyst (0.15 g) was dispersed in it under continuous air bubbling in the dark for 15 min to ensure the establishment of an adsorption/desorption equilibrium prior to photodegradation. Then the mixture was irradiated under UV light in photoreactor with proper aeration. After the required time of reaction, the solution was centrifuged and its absorbance spectra were recorded from 200 to 800 nm using a UV–visible spectrophotometer (Perkin Elmer Lambda-35). The percentage of photodegradation was calculated based on the following equation:

Degradation $(\%) = (1 - (A/A_0)) \times 100$, where A_0 and A represents the absorbance of the initial dye solution and the same after photodegradation. The efficiency of degradation of some other industrial dyes was also investigated over ZnO microflowers.

Results and discussion

The preparation of highly efficient and morphology controlled nano or micro material is a challenging task in materials research. A wide variety of synthesis methods have been reported for the synthesis of nanostructured and morphology controlled ZnO materials. Compared to the conventional methods, simplified synthesis procedures always have a prominent seat. In this work, we applied the direct thermal decomposition of previously grinded zinc nitrate hexahydrate for the development of novel crystalline ZnO microflowers. The deliquescent nature and low melting point (36.4 °C) of the precursor makes the grinded material to a liquid phase and its calcination was done directly without the aid of any structure directing agents. The as-obtained ZnO crystals have well-featured flower-like morphology with high photocatalytic activity for dye pollutant degradation. In comparison with the previous reports, ZnO microflowers obtained by the present method proved its best heterogeneous characteristics and the method takes a substantial role for its attractive morphology, simplicity, fast performance and cost-effectiveness.

Characterization of ZnO microflowers

Fig. 1 represents the TGA/DSC curves of the nitrate precursor, $Zn(NO_3)_2{\cdot}6H_2O$. The precursor was thermally scanned from 30 to 600 °C with a slow heating rate of 4 °C min^{-1} using helium as the carrier gas. In the TGA plot, the two continuous adjacent weight losses were noted with a total of 72 %. The first weight loss up to 220 °C was attributed to the loss of water of crystallization from the nitrate precursor and the second mass loss from 290 to 350 °C was due to the thermal decomposition of nitrate precursor to zinc oxide with the liberation of nitrogen oxides [41]. Similar results were also noticed in the DSC plot. In the DSC plot, the endothermic peaks noted at around 38 and 125 °C were corresponded to the melting and boiling point or the decomposition temperature of the nitrate precursor. The decomposition proceeds till 350 °C. The endothermic peak at ~330 °C in the DSC curve was ascribed to the weight loss corresponding to the decomposition of zinc(II) nitrate to pure ZnO. After 350 °C, there is no weight loss in the sample, indicating the complete transformation of nitrate precursor to ZnO. Thus it is clear that only 350 °C was required for the complete pyrolysis of the nitrate precursor to ZnO. In our studies, we selected a slightly higher pyrolysis temperature of 400 °C to ensure the complete conversion. A higher calcination temperature of 600 °C was also performed for the synthesis, to study its effect on the properties and activities of ZnO.

Powder X-ray diffraction patterns of the calcined samples are shown in Fig. 2. The diffraction patterns at the 2θ values 31.7°, 34.1°, 36.2°, 47.5°, 56.5°, 62.8°, 67.9°, 69.0° and 72.5° can be indexed to the hexagonal wurtzite structure of ZnO with $P6_3mc$ space group (JCPDS: 01-089-0511), irrespective of the calcination temperature, which is the exclusive phase present in the as-synthesised ZnO materials. The sharp and intense diffraction peaks confirmed the high crystalline quality of the ZnO. The synthesis temperature has slightly affected the crystallite size of ZnO. ZnO prepared at 400 °C has the crystallite size of ~47 nm, whereas the sample calcined at 600 °C showed a crystallite size of ~50 nm. This slight increase in the crystalline size may be due to the much higher nuclear growth rate of crystallites at high temperatures [42, 43].

The FT-IR spectra of ZnO crystals are shown in Fig. 3. The intense and broad band centered at around 475 cm^{-1} in the spectra was attributed to the characteristic stretching vibration of Zn–O bond in transmission mode [44, 45]. The absence of any other prominent peaks indicates the lack of adsorbed surface impurities.

The surface morphologies of the as-synthesized ZnO samples were studied with the help of SEM images and the results are shown in Fig. 4. It is reported that the zinc(II) nitrate sintering produces hexagonal pyramids instead of flowers [46], but in the present case, flower-like morphology was observed for ZnO. Hexagonal pyramids form the basic unit of such microflowers and which are aggregated three dimensionally for the formation of microflowers. The hexagonal pyramids in the ZnO microflower have well separated six triangular faces and a sharp end tip at the top, characteristic of the normal pyramids obtained by the direct pyrolysis of the nitrate precursor [47]. The microflowers were formed in such a way that many of the hexagonal pyramids joined together through the hexagonal bottom portion and

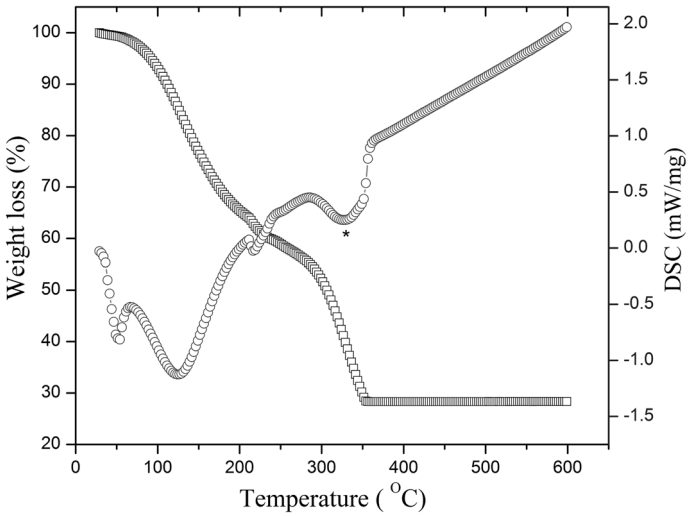

Fig. 1 TGA/DSC curves of zinc nitrate hexahydrate

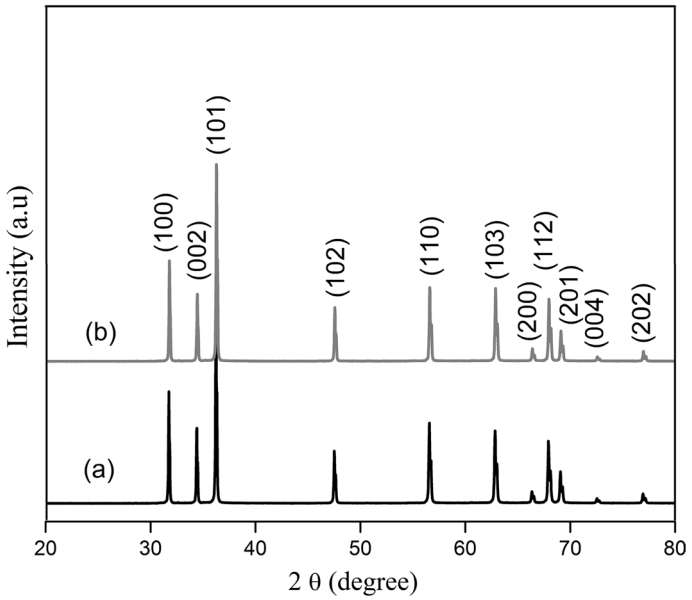

Fig. 2 XRD pattern of the samples at (*a*) 400 °C, (*b*) 600 °C

which forms the center of microflower and the pyramidal end was oriented outwards like the petals of a flower. Also from Fig. 4, it is visibly evident that even though the size of the microflowers was different; the size of hexagonal pyramid is found to be almost same with average size varying from 10 to 15 μm. Some studies reported the

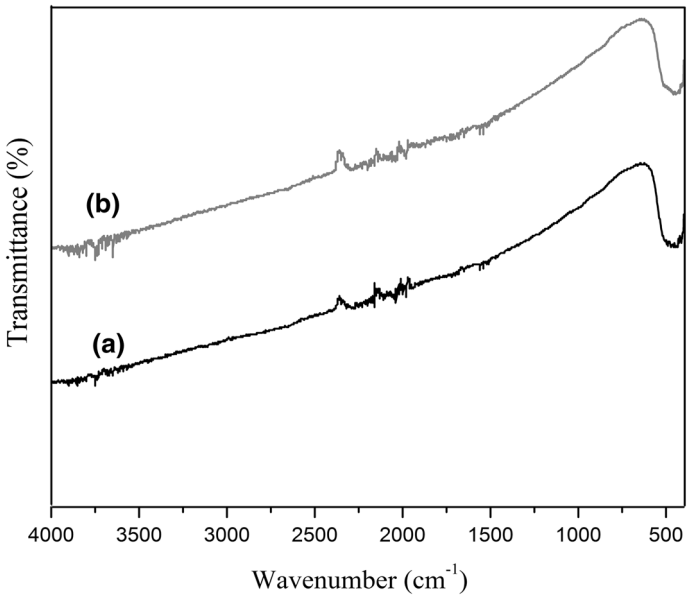

Fig. 3 FT-IR spectra of ZnO calcined at (*a*) 400 °C, (*b*) 600 °C

use of additional reagents such as KI or hydrazine for the formation of flower like morphologies from single units [48–50]. However, in our case, we ruminate that the initial melting happened by the grinding followed deliquescence of the precursor and the oriented growth during the calcination, reasons the step growth or aggregation of hexagonal micropyramids.

As shown in Fig. 4, the sample calcined at 600 °C shows variety of microflowers with a huge number of hexagonal pyramidal petals. An increase in the synthesis temperature resulted in the formation of microflowers with increased number of hexagonal pyramidal petals. In the first image (Fig. 4a), a highly aggregated flower is shown with a huge number of pyramidal clusters oriented in a three dimensional manner. The average size of this large ZnO microflower was found to be about 100 μm. This type of microflower has been not reported in literatures so far by the ordinary thermal decomposition of the nitrate precursor. ZnO microflowers with lower number of pyramidal petals with size ranging from 10 μm to 70 μm were also observed at the same calcination temperature. At a lower annealing temperature of 400 °C, flower-like structures were observed as shown in Fig. 4c, with the same basic hexagonal pyramidal petal units; but the observed change was in the low number of pyramidal petals in the flowers, which may be due to the lower aggregation rate of pyramidal petals compared to that at 600 °C. In addition to the microflowers, star shaped microstructures were also noticed at 400 °C as seen in Fig. 4d. The inset of Fig. 4d shows the magnified image of a single hexagonal pyramidal petal in the flower, which is oriented in a single direction.

Thus, it is clear that the flower growth or pyramidal aggregation was more pronounced at 600 °C because a large flower with the approximate size of 100 μm

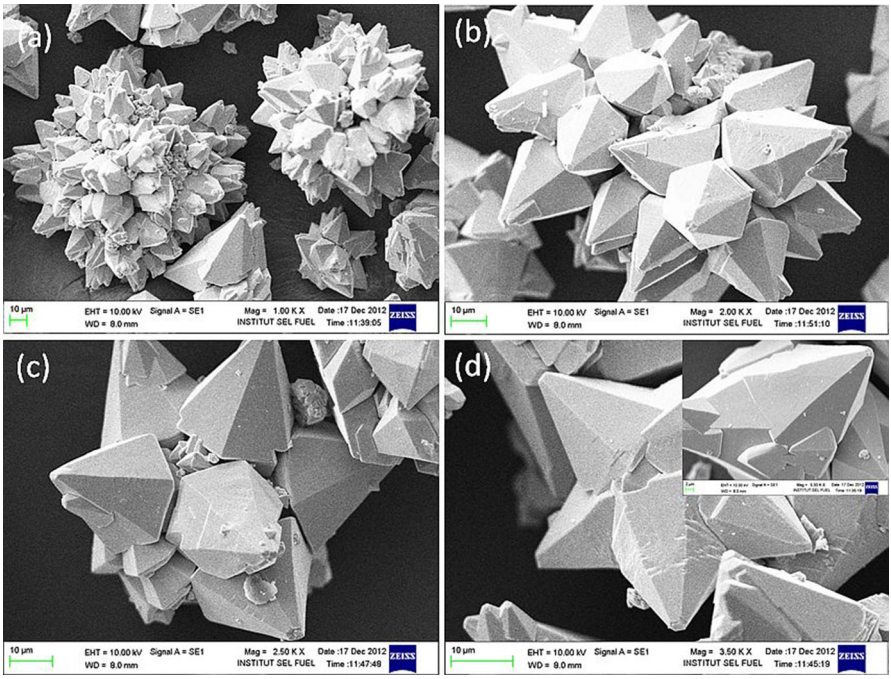

Fig. 4 SEM images of ZnO microflowers **a**, **b** calcined at 600 °C **c**, **d** calcined at 400 °C

was formed by the rapid aggregation of hexagonal micropyramids. However, at a lower temperature of 400 °C, the agglomeration rate was found to be low compared to 600 °C. This may be the reason for the formation microflowers with low number of pyramidal petal combs. Saravanan et al. [40] found that the calcination temperature has a great role in the morphology of the ZnO nanorods obtained by the thermal decomposition of the acetate precursor and reported that at higher calcination temperatures, their nanorods changed to irregular shape, but in our case, even at a higher calcination temperature of 600 °C, the flower-like morphology was preserved, indicating the morphology preservation at high temperatures. The step growth for the formation of microflower bundles was increased with the calcination temperature.

Fig. 5 shows the TEM image of the ZnO microflower at 600 °C, where highly dense and aggregated hexagonal pyramids were visibly clear. The inset figure in Fig. 5a represents the selected area electron diffraction pattern of the single pyramidal unit in the microflower. SAED pattern shows the sharp and bright diffraction spots indicating the single crystalline nature of the pyramid petal unit and the growth direction can be indexed along the c-axis or [0001] direction [51]. The TEM-EDX analysis of ZnO microflowers was also carried out (Fig. 5b). From this spectrum, it is seen that the ZnO microflower contains only Zn and O, without any other elements. The signal of Cu originates from the copper grid used for viewing TEM images and the signal of C was due to the thin carbon film on Cu grid.

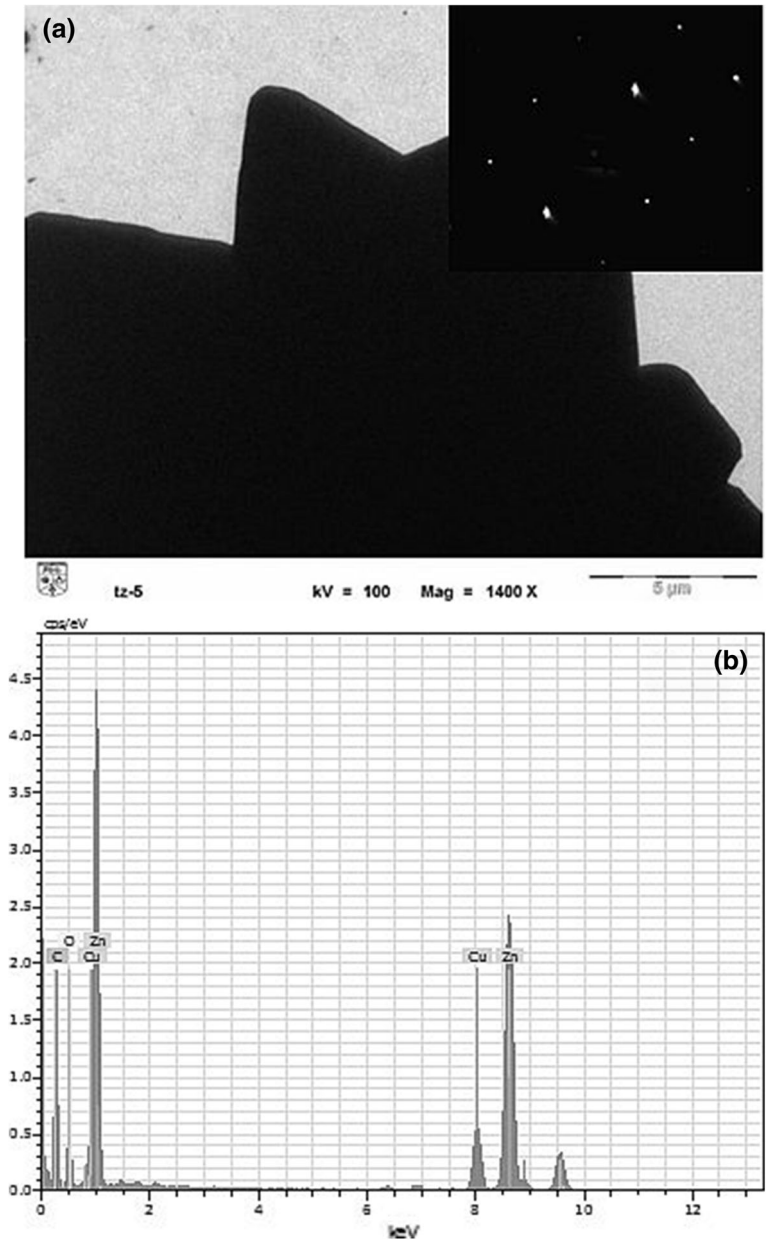

Fig. 5 TEM image of **a** ZnO microflower at 600 °C and its SAED pattern (*inset figure*), **b** EDX pattern

As ZnO is a polar crystal [52], it prefers the growth in polar axis i.e. along the [0001] direction or c-axis as shown in the SAED pattern. The continuous growth along this direction can occur by the adsorption of growth units on this [0001] facet and which results in the formation of one dimensional hexagonal nanorod [53]. Due to the

adsorption of impure groups on this plane, the hindering of growth unit attachment takes place and the crystal growth has been retarded along this facet. The formation of hexagonal pyramid-like petal structures in the ZnO microflower was due to the attachment of nitrate ions on the facet [46, 47]. More clearly, the nitrate ions adsorb on the polar plane and which retards the rapid growth of ZnO and a sharp end at the c-axis takes place, resulting in the formation of hexagonal pyramids [54, 55].

Photocatalytic degradation of methylene blue

The photocatalytic activity of the as-prepared ZnO microflowers was investigated using the photodegradation of methylene blue under UV light irradiation. Additionally, we did some experiments to confirm the degradation effectiveness of ZnO microflowers for other industrial dyes. For the photocatalytic oxidation process, we supplied air as the potential oxidizing agent, until the dye solution became completely degraded (colorless). 2 % self-degradation of methylene blue (noncatalytic dye degradation) was noted when the reaction was conducted in the absence of ZnO photocatalysts and under UV irradiation. ZnO microflowers prepared by the thermal decomposition method have a considerable role in the permanent removal of dyes from waste water by the use of UV irradiation, because the as-synthesized ZnO presented a negligible adsorption (<1 %) in the dark reaction [56–58]. Therefore, exclusive photocatalytic degradation was resulted over the ZnO microflowers.

We performed the degradation of MB solution over ZnO microflowers obtained at 400 and 600 °C; where 98.5 % dye degradation was noted for both samples within 60 min, which indicates that both samples show almost the same activity due to their close crystallinity and the well-defined flower-like morphology. The reaction was performed under the conditions of 50 mL of 5 mg/L concentration of methylene blue solution with a catalyst dosage of 150 mg. To study the effect of various parameters such as illumination time, catalyst weight, initial dye concentration, volume etc., we selected ZnO calcined at 400 °C as the photocatalyst and methylene blue as the model dye pollutant. Fig. 6 shows the photodegradation efficiency of ZnO calcined at 400 °C with time over a catalyst dosage of 150 mg. Over the photocatalyst, around 99 % degradation was achieved within 60 min and after that no increment was observed while doing the reaction for further time. Fig. 7a shows the effect of catalyst dosage on the photodegradation efficiency. An increase in the catalyst weight exhibited a positive effect in the degradation rate as shown in the plot, and within 45 min, 97 % degradation was observed for the dye solution over 0.30 g ZnO. An increase in the amount of ZnO photocatalysts provides more photoactive sites to absorb the UV light, so that the time required for the methylene blue degradation was decreased [59]. Fig. 7b shows the effect of volume of dye solution on the degradation efficiency and noted that with increase in the volume of dye solution, the degradation rate was decreased, since only the same amount of catalyst was available for more dye molecules. As we expected, the initial dye concentration has a significant role in the degradation rate of dye solution and observed that, with an increase in the initial dye concentration, the rate of degradation decreased drastically. 37, 45, 88 and 99 % degradation was observed for 20, 15, 10 and 5 mg/L dye concentrations in 2 h of reaction time as shown in Fig. 7c.

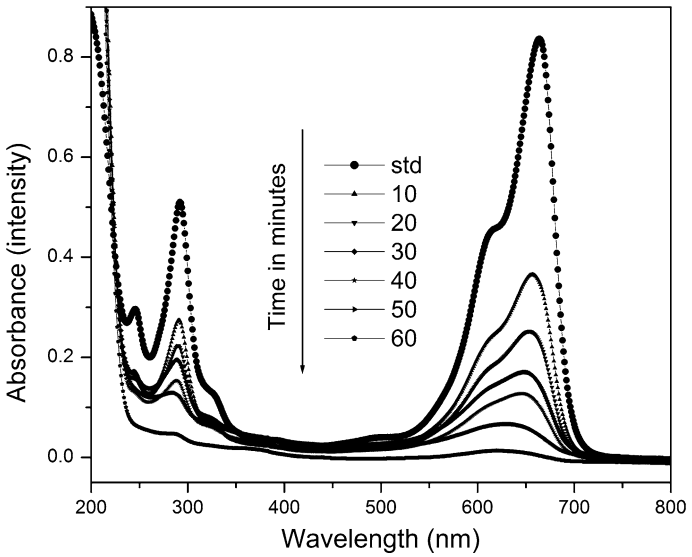

Fig. 6 Change in absorbance spectra of methylene blue dye solution with time (50 mL 5 mg/L dye solution, 0.15 g ZnO at 400 °C with constant air bubbling)

Many of the photocatalysts have not been useful for further photodegradation experiments due to the deactivation of the catalyst. But over the prepared ZnO microflowers, we have done several experiments to prove its reusability. ZnO photocatalysts left after the degradation experiments were washed, filtered, dried and calcined before it is used for next run. Fig. 8 represents the reusability data for the ZnO photocatalysts. From the figure, it is evident that the microflowers have high reusability for seven consecutive runs, which depicts the high photostability of the catalysts against photocorrosion [26]. We also compared the photocatalytic activity of ZnO microflowers with commercial grade ZnO for methylene blue degradation and found that commercial grade ZnO was more active than ZnO microflowers. Within 6 min, 100 % degradation was noted in the case of commercial ZnO, but we faced a separation difficulty while using it for the reaction, due to its lower sedimentation power because of the fine powder nature [60]. This enhances the use of ZnO microflowers as heterogeneous photocatalysts. Table 1 represents the efficiency of degradation of various industrial dye pollutants over ZnO microflowers calcined at 400 °C. It was clear that more than 70 % of all of the organic dyes studied were degraded within 60 min under UV-light irradiation. Complete degradation of malachite green was noted within 60 min over the present catalyst, but only 73 % degradation was noted for the methyl orange dye solution. The high catalytic activity of the prepared ZnO microflowers for the photooxidation process may be attributed to the crystallinity of ZnO samples [20, 40].

The photoactive ZnO microflowers were synthesized by a method easy to perform: thermal decomposition of previously melted nitrate precursor without any special care and procedures. Therefore, this is encouraged for its bulk production.

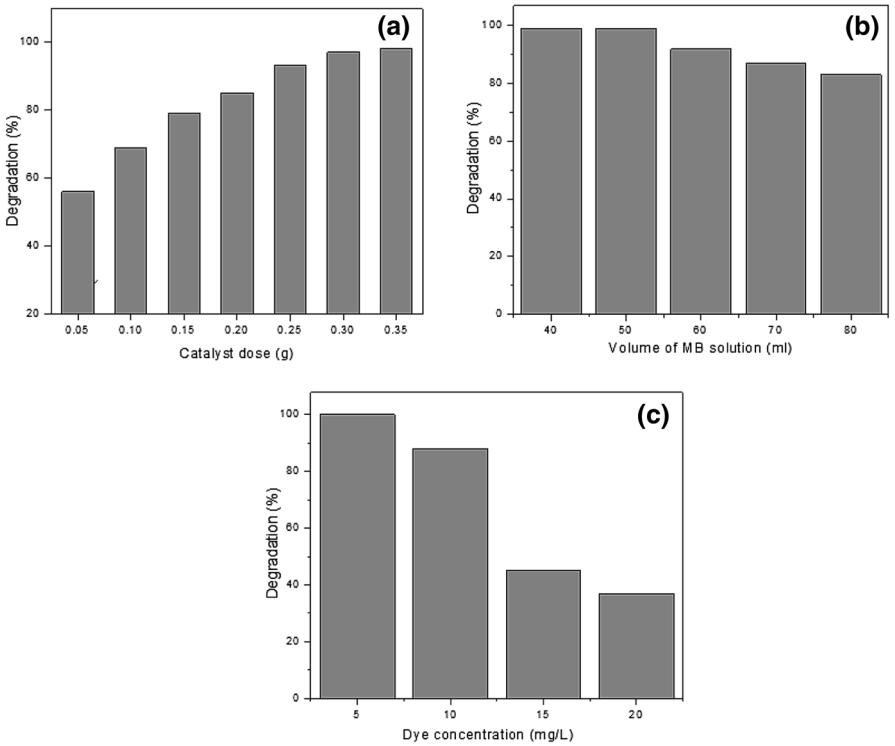

Fig. 7 **a** Effect of catalyst dosage (50 mL 5 mg/L dye solution, 45 min UV irradiation with constant air bubbling), **b** Effect of volume of dye solution (0.15 g ZnO at 400 °C, 60 min UV irradiation with constant air bubbling), and **c** Effect of initial dye concentration (50 mL dye solution, 0.15 g ZnO at 400 °C, 120 min UV irradiation with constant air bubbling)

The method is found to be simple and efficient compared to the solvent-based conventional wet methods and other tedious methods previously reported in literature, in terms of its morphology and degradation capacity. In comparison with literature reports, ZnO prepared by the pyrolysis of precursor enhanced the degradation efficiency and the method of preparation is substantial for its best characteristics such as simplicity, cost-effectiveness, rapid synthesis and also for the formation of well oriented flower like morphology.

Conclusion

Highly oriented three dimensional ZnO microflowers have been successfully fabricated by the direct thermal decomposition of the previously grinded/melted nitrate precursor at two different calcination temperatures of 400 and 600 °C, without the use of any structure directing agents or surfactants. The as-synthesized ZnO microflowers were characterized by means of various analytical techniques. X-ray diffraction studies confirmed the phase pure hexagonal wurtzite crystalline

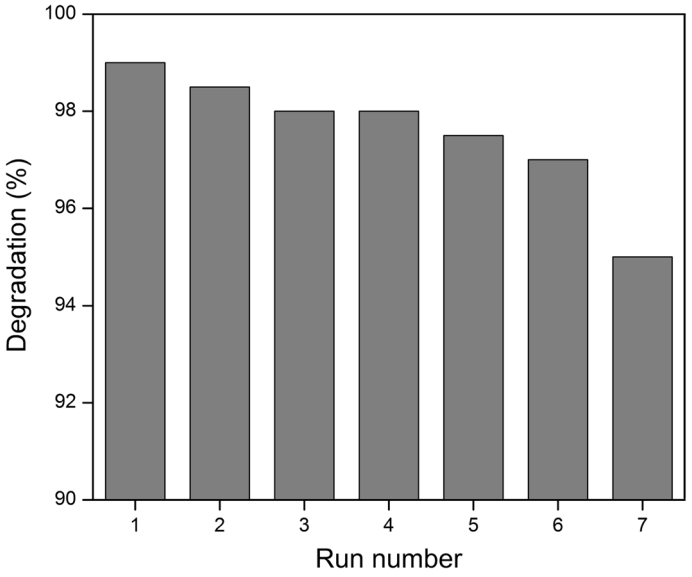

Fig. 8 Reusability of ZnO microflowers (50 mL 5 mg/L MB solution 65 min of light irradiation)

Table 1 Catalytic efficiency of ZnO microflowers for the degradation of various organic dye pollutants (50 mL 5 mg/L dye solution, 150 mg ZnO (400 °C), continuous air bubbling for 60 min under UV illumination)

Dye	Degradation (%)
Methylene blue	99
Malachite green	100
Methyl orange	73
Acid blue	80
Congo red	77

structure. SEM and TEM images showed the various microflower and star-like morphology of the prepared samples. Hexagonal pyramids form the fundamental unit of such microflowers, whose regulated aggregation resulted in the formation of 3D microflowers. SAED analysis confirmed the single crystalline nature of the ZnO hexagonal micropyramids. The photocatalytic degradation of hazardous industrial dye pollutants were effectively done over ZnO microflowers. Several concentrations of dye solution were degraded effectively under UV-light irradiation at a low catalyst dosage. Reaction parameters were varied to optimize the degradation conditions and noted that irrespective of the calcination temperature, ZnO microflowers exhibited same degradation efficiency due to their excellent crystallinity. The microflowers exhibited high reusability for dye degradation.

Acknowledgments We acknowledge UKM, DIP-2012-04 and OUP-2012-074 for the financial support and FST, CRIM and FCI for material analysis. Manoj special thanks to University Research Scholarship Scheme, UKM, for the Doctorial fellowship.

References

1. Ye J, Zhou R, Zheng C, Sun Q, Lv Y, Li C, Hou X (2012) Size-controllable synthesis of spherical ZnO nanoparticles: size- and concentration-dependent resonant light scattering. Microchem J 100:61–65
2. Zhang J, Keita B, Nadjo L, Mbomekalle IM, Liu TB (2008) Self-assembly of polyoxometalate macroanion-capped Pd0 nanoparticles in aqueous solution. Langmuir 24:5277–5283
3. Sun G, Cao M, Wang Y, Hu C, Liu Y, Ren L, Pu Z (2006) Anionic surfactant-assisted hydrothermal synthesis of high-aspect-ratio ZnO nanowires and their photoluminescence property. Mater Lett 60:2777–2782
4. Saito N, Haneda H, Sekiguchi T, Ohashi N, Sakaguchi I, Koumoto K (2002) Low-temperature fabrication of light-emitting zinc oxide micro patterns using self-assembled monolayers. Adv Mater 14:418–421
5. Cao H, Xu JY, Zhang DZ, Chang SH, Ho ST, Seelig EW, Liu X, Chang RPH (2000) Spatial confinement of laser light in active random media. Phys Rev Lett 84:5584–5587
6. Pan ZW, Dai ZR, Wang ZL (2001) Nanobelts of semiconducting oxides. Science 291:1947–1949
7. Park JS, Lee BR, Lee JM, Kim JS, Kim SO, Song MH (2010) Efficient hybrid organic-inorganic light emitting diodes with self-assembled dipole molecule deposited metal oxides. Appl Phys Lett 96:243306–243308
8. Mitra P, Chatterjee AP, Maiti HS (1998) Chemical deposition of ZnO films for gas sensors. J Mater Sci 9:441–445
9. Law M, Greene LE, Johnson JC, Saykally R, Yang PD (2005) Nanowire dye-sensitized solar cells. Nat Mater 4:455–459
10. Devancy WE, Chen WS, Stewart JM, Mickelsen RA (1990) IEEE Trans Electron Dev 37:428–433
11. Wang Y, Li X, Wang N, Quan X, Chen Y (2008) Controllable synthesis of ZnO nanoflowers and their morphology-dependent photocatalytic activities. Sep Purif Technol 62:727–732
12. Suwanboon S, Amornpitoksuk P, Muensit N (2011) Dependence of photocatalytic activity on structural and optical properties of nanocrystalline ZnO powders. Ceram Int 37:2247–2253
13. Look DC, Reynolds DC, Hemsky Jones RL, Sizelove JR (1999) Production and annealing of electron irradiation damage in ZnO. Appl Phys Lett 75:811–813
14. Arnold MS, Avouris P, Pan ZW, Wang ZL (2003) Field-effect transistors based on single semiconducting oxide nanobelts. J Phys Chem B 107:659–663
15. Park WI, Jun YH, Jung SW, Yi JC (2003) Excitonic emissions observed in ZnO single crystal nanorods. Appl Phys Lett 82:964–966
16. Lee J, Wang JH, Mashek TT, Mason TO, Miller AE, Siegel RW (1995) Impedance spectroscopy of grain boundaries in nanophase ZnO. J Mater Res 10:2295–2300
17. Lu Y, Wang L, Wang D, Xie T, Chen L, Lin Y (2011) A comparative study on plate-like and flower-like ZnO nanocrystals surface photovoltage property and photocatalytic activity. Mater Chem Phys 129:281–287
18. Waugh MR, Hyett G, Parkin IP (2008) Zinc oxide thin films grown by aerosol assisted CVD. Chem Vap Deposition 14:366–372
19. Lee SD, Nam SH, Kim MH, Boo JH (2012) Synthesis and photocatalytic property of ZnO nanoparticles prepared by spray-pyrolysis method. Phys Procedia 32:320–326
20. Saravanan R, Karthikeyan S, Gupta VK, Sekaran G, Narayanan V, Stephen A (2013) Enhanced photocatalytic activity of ZnO/CuO nanocomposite for the degradation of textile dye on visible light illumination. Mater Sci Eng C 33:91–98
21. Han Z, Liao L, Wu Y, Pan H, Shen S, Chen J (2012) Synthesis and photocatalytic application of oriented hierarchical ZnO flower-rod architectures. J Hazard Mater 217–218:100–106
22. Rai P, Song HM, Kim YS, Song MK, Oh PR et al (2012) Microwave assisted hydrothermal synthesis of single crystalline ZnO nanorods for gas sensor application. Mater Lett 68:90–93
23. Zhong J, Li J, Xiao Z, Hu W, Zhou X, Zheng X (2013) Improved photocatalytic performance of ZnO prepared by sol–gel method with the assistance of CTAB. Mater Lett 91:301–303
24. Marto J, Marcos PS, Trindade T, Labrincha JA (2009) Photocatalytic decolouration of Orange II by ZnO active layers screen-printed on ceramic tiles. J Hazard Mater 163:36–42
25. Sangari NU, Devi SC (2013) Synthesis and characterization of nano ZnO rods via microwave assisted chemical precipitation method. J Solid State Chem 197:483–488

26. Pudukudy M, Yaakob Z (2014) Facile solid state synthesis of ZnO hexagonal nanogranules with excellent photocatalytic activity. Appl Surf Sci 292:520–530
27. Pudukudy M, Yaakob Z, Narayanan B, Gopalakrishnan A, Tasirin SM (2013) Facile synthesis of bimodal mesoporous spinel Co_3O_4 nanomaterials and their structural properties. Superlattices Microstruct 64:15–26
28. Lu Y, Wang L, Wang D, Xie T, Chen L, Lin Y (2011) A comparative study on plate-like and flower-like ZnO nanocrystals surface photo voltage property and photocatalytic activity. Mater Chem Phys 129:281–287
29. Yu H, Ming H, Zhang H, Li H, Pan K et al (2012) Au/ZnO nanocomposites: facile fabrication and enhanced photocatalytic activity for degradation of benzene. Mater Chem Phys 137:113–117
30. Lei A, Qu B, Zhou W, Wang Y, Zhang Q, Zou B (2012) Facile synthesis and enhanced photocatalytic activity of hierarchical porous ZnO microspheres. Mater Lett 66:72–75
31. Venkatesha TG, Nayaka YA, Viswanatha R, Vidyasagar CC, Chethana BK (2012) Electrochemical synthesis and photocatalytic behavior of flower shaped ZnO microstructures. Powder Technol 225:232–238
32. Sun F, Qiao X, Tan F, Wang W, Qiu X (2012) Fabrication and photocatalytic activities of ZnO arrays with different nanostructures. Appl Surf Sci 263:704–711
33. Pudukudy M, Yaakob Z (2013) Hydrothermal synthesis of mesostructured ZnO micropyramids with enhanced photocatalytic performance. Superlattices Microstruct 63:47–57
34. Sheng WS, Ming JQ, Lin SY, Yun SS, Hong JL, Ming WY (2012) Microwave-hydrothermal preparation of flower-like ZnO microstructure and its photocatalytic activity. Trans Nonferrous Met Soc China 22:2465–2470
35. Liu Y, Lu H, Li S, Xing X, Xi G (2012) Preparation and photocatalytic property of hexagonal cylinder-like bipods ZnO microcrystal photocatalyst. Dyes Pigm 95:443–449
36. Mahmud S (2011) One-dimensional growth of zinc oxide nanostructures from large micro- particles in a highly rapid synthesis. J Alloys Compd 509:4035–4040
37. Delgado GT, Romero CIZ, Hernadez SAM, Perez RC, Angel OZ (2009) Optical and structural properties of the sol–gel-prepared ZnO thin films and their effect on the photocatalytic activity. Sol Energy Mater Sol Cells 93:55–59
38. Anandan S, Vinu A, Mori T, Gokulakrishnan N, Srinivasu P, Murugesan V, Arig K (2007) Photocatalytic degradation of 2,4,6-trichlorophenol using lanthanum doped ZnO in aqueous suspension. Catal Commun 8:1377–1382
39. Beydoun D, Amal R, Low GKC, McEvoy S (2000) Novel photocatalyst: Titania coated magnetite: activity and photo dissolution. J Phys Chem B 104:4387–4396
40. Saravanan R, Thirumal E, Gupta VK, Narayanan V, Stephen A (2013) The photocatalytic activity of ZnO prepared by simple thermal decomposition method at various temperatures. J Mol Liq 177:394–401
41. Kang SZ, Wu T, Li X, Mu J (2010) A facile gelatin-assisted preparation and photocatalytic activity of zinc oxide nanosheets. Colloids Surf A 369:268–271
42. Dakhlaoui A, Jendoubi M, Smiri LS, Kanaev A, Jouini N (2009) Synthesis, characterization and optical properties of ZnO nanoparticles with controlled size and morphology. J Cryst Growth 311:3989–3996
43. Leoni M, Maggio RD, Polizzi S, Scardi P (2004) X-ray diffraction methodology for the microstructural analysis of nanocrystalline powders: application to cerium oxide. J Am Ceram Soc 87:1133–1140
44. Pudukudy M, Yaakob Z (2014) Simple chemical synthesis of novel ZnO nanostructures: role of counter ions. Solid State Sci 30:78–88
45. Gu F, Wang SF, Lu MK, Zhou GJ, Xu D, Yuan DR (2004) Structure evaluation and highly enhanced luminescence of Dy^{3+}–Doped ZnO nanocrystals by Li^{+} doping via combustion method. Langmuir 20:3528–3531
46. Merceroz GP, Thierry R, Jouneau PH, Ferret P, Feuillet G (2012) Compared growth mechanisms of Zn-polar ZnO nanowires on O-polar ZnO and on sapphire. Nanotechnol 23:125702
47. Joo J, Chow BY, Prakash M, Boyden ES, Jacobson JM (2011) Face-selective electrostatic control of hydrothermal zinc oxide nanowire synthesis. Nat Mater 10:596–601
48. Zou GF, Yu DB, Wang DB, Zhang WQ, Xu LQ, Yu WC, Qian YT (2004) Controlled synthesis of ZnO nanocrystals with column-, rosette-and fiber-like morphologies and their photoluminescence property. Mater Chem Phys 88:150–154

49. Peng W, Qu S, Cong G, Wang Z (2006) Synthesis and structures of morphology-controlled ZnO Nano- and microcrystals. Cryst Growth Des 6:1518–1522
50. Chen Y, Yu R, Shi Q, Qin J, Zheng F (2007) Hydrothermal synthesis of hexagonal ZnO clusters. Mater Lett 61:4438–4441
51. Zhu Z, Yang D, Liu H (2011) Microwave-assisted hydrothermal synthesis of ZnO rod-assembled microspheres and their photocatalytic performances. Adv Powder Technol 22:493–497
52. Wang D, Song (2005) Controllable synthesis of ZnO nanorod and prism arrays in a large area. J Phys Chem B 109:12697–12700
53. Wang Y, Fan X, Sun J (2009) Hydrothermal synthesis of phosphate-mediated ZnO nanosheets. Mater Lett 63:350–352
54. Pawar RC, Cho D, Lee CS (2013) Fabrication of nanocomposite photocatalysts from zinc oxide nanostructures and reduced graphene oxide. Curr Appl Phys 13:S50–S57
55. Zhang Z, Mu J (2007) Hydrothermal synthesis of ZnO nano bundles controlled by PEO–PPO–PEO block copolymers. J Col Interface Sci 307:79–82
56. Esfahani MN, Nourmohammadi A (2012) ZnO/ITO interface nanostructure films for the photocatalytic degradation of a textile dye. Reac Kinet Mech Cat 107:79–88
57. Pudukudy M, Yaakob Z (2014) Sol–gel synthesis, characterisation, and photocatalytic activity of porous spinel Co_3O_4 nanosheets. Chem Pap. doi: 10.2478/s11696-014-0561-7
58. Karunakaran C, Rajeswari V, Gomathisankar P (2011) Optical, electrical, photocatalytic, and bactericidal properties of microwave synthesized nanocrystalline Ag–ZnO and ZnO. Solid State Sci 13:923–928
59. Fatimah I, Wang S, Wulandari D (2011) ZnO/montmorillonite for photocatalytic and photochemical degradation of methylene blue. Appl Clay Sci 53:553–560
60. Amornpitoksuk P, Suwanboon S, Sangkanu S, Sukhoom S, Muensit S (2012) Morphology, photocatalytic and antibacterial activities of radial spherical ZnO nanorods controlled with a diblock copolymer. Superlattices Microstruct 51:103–113